MOLECULAR AND CELLULAR BIOLOGY, Sept. 2004, p. 7636–7642 Vol. 24, No. 17
0270-7306/04/$08.00+0 DOI: 10.1128/MCB.24.17.7636–7642.2004

Cell Depletion Due to Diphtheria Toxin Fragment A after Cre-Mediated Recombination

Damian Brockschnieder,[1] Corinna Lappe-Siefke,[1,2] Sandra Goebbels,[2] Michael R. Boesl,[1,3] Klaus-Armin Nave,[2] and Dieter Riethmacher[1]*

Zentrum für Molekulare Neurobiologie, Universität Hamburg, Hamburg,[1] Max Planck Institute for Experimental Medicine, Göttingen,[2] and Max Planck Institute of Neurobiology, Martinsried,[3] Germany

Received 19 February 2004/Returned for modification 19 April 2004/Accepted 27 May 2004

Abnormal cell loss is the common cause of a large number of developmental and degenerative diseases. To model such diseases in transgenic animals, we have developed a line of mice that allows the efficient depletion of virtually any cell type in vivo following somatic Cre-mediated gene recombination. By introducing the diphtheria toxin fragment A (DT-A) gene as a conditional expression construct (floxed *lacZ*–DT-A) into the ubiquitously expressed ROSA26 locus, we produced a line of mice that would permit cell-specific activation of the toxin gene. Following Cre-mediated recombination under the control of cell-type-specific promoters, *lacZ* gene expression was efficiently replaced by de novo transcription of the Cre-recombined DT-A gene. We provide proof of this principle, initially for cells of the central nervous system (pyramidal neurons and oligodendrocytes), the immune system (B cells), and liver tissue (hepatocytes), that the conditional expression of DT-A is functional in vivo, resulting in the generation of novel degenerative disease models.

The exact regulation of proliferation and cell death is important for the maintenance of tissue homeostasis, and its deregulation contributes to such diverse processes as autoimmune disease, immunodeficiency, tumorigenesis, and neurodegeneration. Cell loss as a consequence of either necrosis or programmed cell death is commonly observed in diseased tissues, leading to a clinically overt phenotype when the affected tissue is no longer able to function adequately (31). For example, in the central nervous system the loss of 50 to 70% of specific dopaminergic striatal neurons results in Parkinson's disease (22), loss of enteric ganglion cells causes Hirschsprung's disease (1), and loss of B cells is a hallmark of AIDS (8). Thus, a system to specifically and desirably delete cells of any lineage and at any given time would be an important tool for modeling human diseases of various etiologies. Not only could progressive tissue degeneration be studied in such a system but processes like endogenous regeneration and repair as well as the employment of stem cells to replace the diseased tissue could also be examined.

The conditional expression of the diphtheria toxin fragment A (DT-A) gene was chosen as an approach to establish such a system, as the exact mode of its action is known (6). Diphtheria toxin is secreted by pathogenic strains of *Corynebacterium diphtheriae* as a single polypeptide that can be converted into two fragments, termed A and B. The A fragment inactivates elongation factor 2 via addition of the ADP-ribose moiety of NAD^+ to a modified histidine residue (7). So the toxicity of diphtheria toxin is critically dependent on the enzymatic activity encoded by the A fragment, and its expression within a cell leads to cell death, as no further activation steps are needed (27). This makes DT-A an attractive tool for the specific elimination of cells.

* Corresponding author. Mailing address: Zentrum für Molekulare Neurobiologie, Falkenried 94, 20251 Hamburg, Germany. Phone: 49 40 428035354. Fax: 49 40 428035359. E-mail: drieth@zmnh.uni-hamburg.de.

We combined the expression of a toxin gene with the new conditional genetic tools employing Cre recombinase. Cre is a member of a large family of recombinases, which has been shown to function in mouse cells in vitro and in vivo and is now widely used in mouse genetics (2, 18, 26). The enzyme recognizes *loxP* sites that consist of a 34-bp sequence motif and excises a DNA segment that is flanked by two of these sites in the same orientation, leaving a single *loxP* site behind (14). In our construct, the *loxP*-flanked *lacZ* open reading frame (ORF) is inserted into the DT-A ORF after the ATG of DT-A, thus allowing the expression of the toxic gene product after excision of the *lacZ* gene (13). We generated a transgenic mouse strain that ubiquitously expresses the floxed *lacZ*–DT-A (*lacZ*^{flox}–DT-A) cassette from the ROSA26 locus. This locus was chosen because it combines ubiquitous expression with a high level of targeting frequency (3, 12, 36). To study the characteristics of the system, we crossed this R26:LacZ/DT-A line with different tissue-specific Cre lines (Alfp-Cre [16], CD19-Cre [29], Nex-Cre [33], and CNP-Cre [19]). We found specific depletions of hepatocytes, B cells, cortical neurons, and myelinating glia, respectively, thereby demonstrating the broad applicability of our system.

MATERIALS AND METHODS

Construction of targeting vector and generation of the R26:LacZ/DT-A line. Targeting the ROSA26 locus was accomplished on the basis of plasmid pROSA26-1 by a knock-in strategy essentially as previously described (36). We inserted a construct consisting of a splice acceptor sequence from plasmid pSAβgeo (12), a *lacZ*^{flox}–DT-A cassette that was identical to the one described previously (13), and a PGK-Neo resistance cassette, in both orientations, into a unique XbaI site of pROSA26-1 to produce two independent mouse lines. The DT-A cassette present in pROSA26-1 was replaced by a herpes simplex virus-thymidine kinase cassette. The linearized targeting vector was introduced by electroporation into line E14.1 embryonic stem (ES) cells. G418- and ganciclovir-resistant ES cell clones were analyzed by Southern blotting with a ^{32}P-labeled 5′ external probe (140 bp) from plasmid pROSA26-5′ (40) (see Fig. 1). Approximately 5% of the analyzed ES cell clones showed a positive recombination event, and two clones (with opposing directions of the PGK-Neo resistance cassette) were injected into C57BL/6 blastocysts and gave rise to germ line

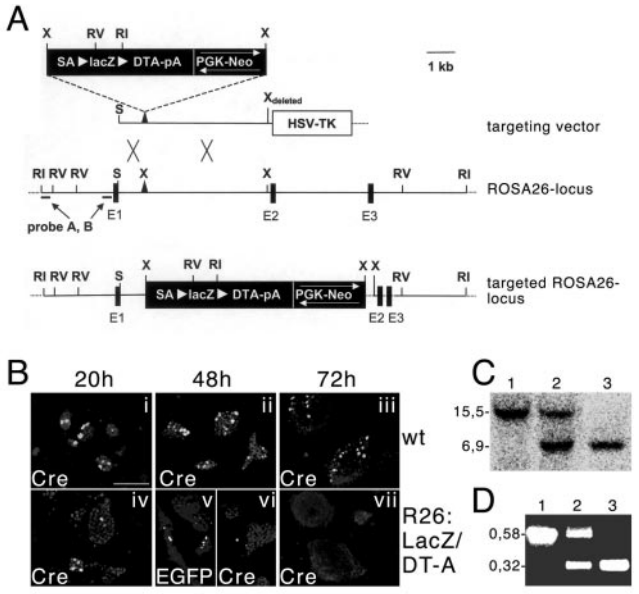

FIG. 1. Targeted integration of the *lacZ*^{flox}–DT-A cassette into the ROSA26 locus. (A) Schematic representation of the targeting strategy employed to achieve expression of *lacZ* under control of the ROSA26 promoter. The targeting vector (top), the wild-type ROSA26 locus (middle), and the targeted ROSA26 locus (bottom) are shown. Restriction sites for EcoRI (RI), EcoRV (RV), XbaI (X), and SacII (S), as well as the location of 5′ probes (probes A and B), are indicated. Black boxes represent exons 1 to 3 (E1 through E3), and white arrowheads flanking the *lacZ*^{flox}–DT-A cassette indicate *loxP* sites. (B) Transfection of wild-type and targeted ES cells with plasmids driving the expression of Cre (i, ii, iii, iv, vi, and vii) or EGFP plus Cre (v). The cells were fixed and monitored for expression of Cre after 20, 48, or 72 h. Note the extinction of the Cre-positive cells after transfection into targeted ES cells after 48 and 72 h. The presence of EGFP, which allows analysis without washing and fixation, at 48 h in some double-transfected mutant cells (v) demonstrates that the almost-complete loss of Cre expression (vi) is partially due to the experimental procedure. Scale bar, 125 μm. (C) Southern blot analysis of DNA from wild-type, heterozygous, and homozygous mutant mice after digestion with EcoRI; the expected sizes of the fragments detected by probe A used for hybridization are indicated (wild type, 15.5 kb; mutant, 6.9 kb). (D) PCR analysis of DNA from wild-type, heterozygous, and homozygous mutant mice; sizes for wild-type (0.58 kb) and mutant (0.32 kb) fragments are indicated.

chimeras. Mice that were heterozygous or homozygous for the desired insertion were genotyped by Southern blotting with a 600-bp PacI-EcoRI probe upstream of the homology region (24) (see Fig. 1). For routine analysis, offspring genotypes were determined by PCR with three oligonucleotides: RosaFA (5′-AAA GTC GCT CTG AGT TGT TAT-3′), RosaRA (5′-GGA GCG GGA GAA ATG GAT ATG-3′), and SpliAcB (5′-CAT CAA GGA AAC CCT GGA CTA CTG-3′) (a wild-type fragment of approximately 580 bp; the mutant fragment was 320 bp). Treatment of animals in this study was in accordance with European guidelines for the care and use of laboratory animals and approved by the Hamburg Animal Care Committees.

Immunohistochemistry, determination of apoptosis, *lacZ* staining, histology, and microscopy. Embryos were isolated from staged pregnancies, and for histological analysis the embryos were fixed in 4% paraformaldehyde (PFA) for up to several days at 4°C, dehydrated, and embedded in Technovit 7100 resin (Kulzer); 4- to 6-μm-thick sections were stained with hematoxylin and eosin or with toluidine blue. For immunohistochemistry, embryos and tissues were fixed in 4% PFA in phosphate-buffered saline (PBS) at 4°C overnight, cryoprotected in 20% sucrose in PBS for 12 h at 4°C, embedded in OCT compound (Miles), and cryosectioned (thickness, 10 μm). Sections were rinsed three times with PBS, blocked for 30 min with PBS containing 0.1% Triton X-100 and 0.2% bovine serum albumin (BSA), and incubated overnight with primary antibodies at 4°C. After being washed three times with PBS (each wash lasting 5 min), the sections were incubated with the appropriate secondary antibodies conjugated to Alexa 466 (Molecular Probes) or Cy3 (Jackson Laboratories; Chemicon) for 1 h. Primary mouse immunoglobulin G1 antibodies were detected with Zenon technology (Molecular Probes). After the sections were rinsed with PBS and nuclei were counterstained with 4′,6′-diamidino-2-phenylindole (DAPI) (0.001 mg/ml of PBS), sections were examined with a Zeiss Axioplan 2 microscope, and images were taken with a Zeiss AxioCam digital camera. The following antibodies were used in this study: rabbit anti-Cre (1:3,000; Babco), mouse anti-glial-fibrillary-acidic protein (anti-GFAP) (1:400; Sigma), mouse anti-NF160 (1:50; Sigma), rat anti-myelin basic protein (anti-MBP) (1:200; Chemicon), and mouse anti-myelin-associated glycoprotein (anti-MAG) (1:200, Chemicon). Sciatic nerves were fixed in 4% PFA in PBS and 1% glutaraldehyde for several days, postfixed, contrasted with 1% OsO_4, and embedded in Epon. For light microscopy, nerve sections (0.5 μm thick) were stained with methylene blue. Preparation for electron microscopy was done essentially as previously described (38). For *lacZ* staining, tissues were fixed by overnight immersion in 1% PFA at 4°C, embedded in 3% agarose, cut with a vibratome (200-μm-thick sections), and stained with 5-bromo-4-chloro-3-indolyl-β-D-galactopyranoside (X-Gal) as described previously (21). Cells undergoing apoptosis were detected on cryosections with an Apodetect Fluorescein Plus kit (Appligene) by the terminal deoxynucleotidyltransferase-mediated dUTP-biotin nick end labeling (TUNEL) method according to the manufacturer's instructions. The number of TUNEL-positive hepatocytes was determined by manual counting of at least 500 cells in four randomly chosen microscopic fields per liver analyzed (from four independent mutants and controls).

Measurement of transaminase activity in serum. Blood collected from retinal vessels of mutant and control mice (number of mice [*n*] for each condition, ≥4) was incubated at room temperature to allow clotting. Serum was separated from the blood clots by centrifugation at 2,000 × *g* for 15 min. Both aspartate aminotransferase (AST) and alanine aminotransferase (ALT) levels in serum were determined with an ALAT/GPT kit (Roche, Mannheim, Germany) on a Hitachi 917 analyzer (Tokyo, Japan). The data represent the means of the data obtained from four to six mice per genotype.

Isolation, flow cytometry, and BrdU labeling of B cells. Bone marrow (harvested from the tibiae and femurs) and spleens from mutant and control mice (for each condition, $n \geq 4$) were mechanically separated into PBS containing 0.5% BSA. Lymphocyte suspensions containing 5×10^6 cells were then surface stained with optimal amounts of fluorochrome-conjugated antibodies (CD19, CD45/B220, and Thy1.1; BD Bioscience) for 20 min on ice. Stained cells were acquired with a FACScan or FACSCalibur, and data were analyzed with CELLQuest software (Becton Dickinson). Dead cells were labeled with propidium iodide and excluded from analysis. For enrichment of splenic B cells, B220-positive cells were purified by magnetic cell sorting (MACS) (Miltenyi Biotech) to ≥90% purity. For B-cell turnover studies, experimental mice were fed with 5′-bromo-2′-deoxyuridine (BrdU) (Sigma) in the drinking water (1 mg of BrdU/ml of water) for seven consecutive days. The BrdU solution was light protected and changed daily. The percentage of BrdU-positive splenic B cells was determined with the BrdU Flow kit (BD Bioscience) according to the manufacturer's instructions.

RESULTS AND DISCUSSION

Generation of R26:LacZ/DT-A ES cells and corresponding mouse line. We made use of a construct described by Grieshammer et al. (13), containing a *loxP*-flanked *lacZ* ORF followed by the ORF of DT-A. We added a splice acceptor sequence 5′ of the ORFs and the *neo* cassette from pMCneo poly(A) 3′ and inserted the construct into the ROSA26 genomic sequences provided in pROSA26.1 (Fig. 1A). pROSA26.1-based constructs give high rates of homologous recombination and ubiquitous expression of the integrated gene (36). We generated two constructs with opposing orientations of the *neo* cassette (Fig. 1A). After electroporation of E14.1 ES cells with the linearized constructs, clones where homologous recombination had occurred were identified by Southern blotting with a 5′ external probe (Fig. 1A and data not shown). To verify the functionality of the integrated construct, two clones with opposing orientations of the *neo* cassette were further character-

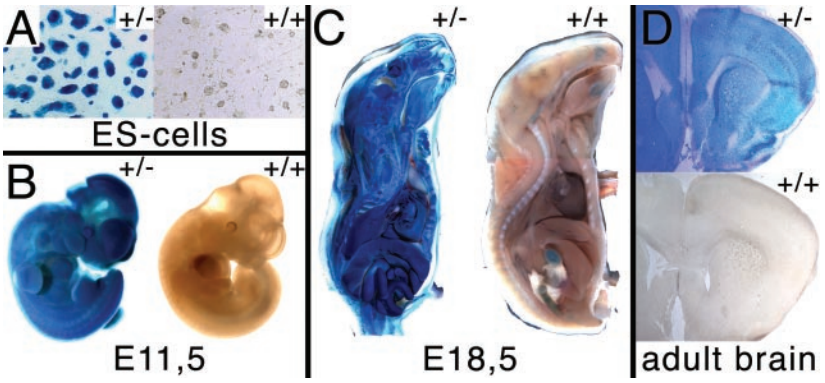

FIG. 2. Monitoring of *lacZ* activity in ES cells, embryos, and adult tissues. (A) Analysis of β-galactosidase activity in R26:LacZ/DT-A (left) and control (right) ES cells. (B) Whole-mount E11.5 R26:LacZ/DT-A embryos (left) were positive for *lacZ*, in contrast to the corresponding control embryo (right). (C) Sagittal section of E18.5 embryos showed ubiquitous expression and activity of *lacZ* in R26:LacZ/DT-A embryos (left) and only restricted background activity in control embryos (right). (D) β-Galactosidase activity in brain isolated from R26:LacZ/DT-A adult animals (top) versus activity in brain tissue isolated from control animals (bottom).

ized in cell culture experiments. We transiently transfected clones with plasmid vectors driving the expression of either enhanced green fluorescent protein (EGFP), Cre recombinase, or both. Transfections from wild-type ES cells with either EGFP or EGFP plus Cre yielded similar amounts of transfectants. Expression was detectable 20 h after transfection, and it was maintained and monitored for the next 52 h. Similar results for EGFP transfections were obtained when we used clones where the *lacZ*^{flox}–DT-A cassette was integrated in the ROSA26 locus, while in experiments where either Cre or EGFP plus Cre was used, expression could be detected 20 h after transfection but then rapidly declined during the next 2 days (Fig. 1B). These experiments demonstrated that after Cre-mediated removal of the *lacZ* ORF, diphtheria toxin becomes active and leads to cell death within 2 to 3 days after its expression. The two tested clones were used to derive germ line chimeras. Heterozygous or homozygous mutant animals were routinely identified by Southern blotting or PCR (Fig. 1C and D). To further characterize the R26:LacZ/DT-A line, we monitored the expression pattern of the *lacZ* marker gene. Beginning with ES cells, we found strong and ubiquitous expression of the *lacZ* gene that was maintained throughout embryogenesis (Fig. 2A through C). As was reported earlier, we also found β-galactosidase activity in every adult tissue examined, exemplified here by adult brain (Fig. 2D) (3, 10, 36).

Cell type-specific depletion with Alfp-Cre and CD19-Cre mice. Having established that the R26:LacZ/DT-A line shows the expected ubiquitous expression of the transgene, we next examined the ability of the toxin gene to undergo Cre-mediated activation and thus depletion of the corresponding cells in living animals. To achieve a liver-specific activation of the toxin, we used the Alfp-Cre line that drives Cre expression by mouse albumin regulatory elements and α-fetoprotein enhancers (16). By using the TUNEL assay, we found a strong increase in cell death in livers from mutant (R26:LacZ/DT-A or Alfp-Cre double-heterozygous) animals compared to cell death in livers from control (R26:LacZ/DT-A or Alfp-Cre single-transgene) animals (Fig. 3A). Consistently, levels in serum of AST and ALT, two abundant liver enzymes that are released into the serum upon liver damage, were five to seven times

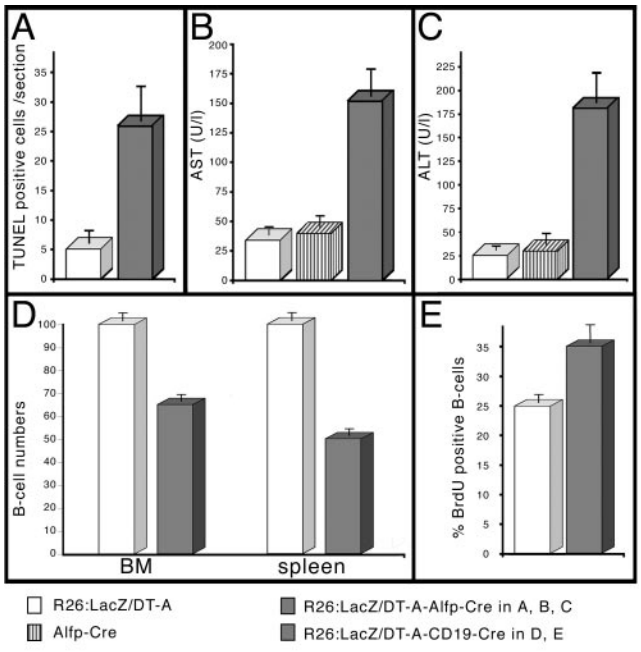

FIG. 3. Serum AST and ALT levels and B-cell reduction; cell depletion in liver and blood. (A) Determination of apoptosis rates by the TUNEL method in liver tissue isolated from 6-week-old control (white column) and mutant (grey column) animals. (B and C) Mean serum activity levels of AST (B) and ALT (C) from 6-week-old animals (number of mice per condition, 4 to 6). White columns, results for single-transgene R26:LacZ/DT-A animals; striped columns, results for single-transgene Alfp-Cre animals; grey columns, results for double-transgene R26:LacZ/DT-A Alfp-Cre animals. The five- to sevenfold increase is statistically significant. (D) Results for the quantification of B-cell (CD19/B220 positive) depletion in lymphocyte preparations of bone marrow (BM) and spleen from control animals (white columns) and mutant animals (grey columns). The control values were in the range of published data and normalized to 100%, compared to 65% in mutant bone marrow or 50% in mutant splenic lymphocyte preparations. (E) Quantification of proliferating, BrdU-positive B cells (B220 positive) isolated from spleen. The 25% increase in proliferating B cells in preparations from mutant (grey columns) animals compared to control (white columns) is statistically significant.

higher in the sera of mutant animals than in the sera of controls (Fig. 3B and C). This elevation of serum AST and ALT levels together with histological findings (data not shown) suggested a toxic hepatosis (17). Closer inspection of Cre expression with Cre-specific antibodies revealed that at a given time point, the protein was detectable only in a subpopulation of hepatocytes (data not shown). Interestingly, Saito et al. also achieved transient hepatotoxicity in mice expressing the diphtheria toxin receptor in hepatocytes after administration of low doses of DT-A (32). So, low doses of toxin or (as in our model) restricted numbers of DT-A-expressing cells in the extremely regenerative liver tissue favor the development of hepatosis rather than acute hepatitis.

Next, we used the CD19-Cre line, where the Cre recombinase ORF is integrated in the CD19 locus to achieve B-cell-specific expression (29). Numbers of B cells in lymphocyte preparations (bone marrow and spleen) of mutant and control mice were compared by flow cytometry with antibodies against B220 and CD19. As illustrated in Fig. 3D, cell fractions in mutant bone marrow and spleen were reduced to 65 and 50%, respectively. CD8/CD4 staining of thymic lymphocytes confirmed that the numbers of T cells were not affected, as expected (data not shown). The reduction in the number of B cells is in good agreement with the recombination efficiencies reported in experiments where the CD19-Cre mouse line was used and the mediated recombination had a negative effect on B-cell survival (15, 28). There are two possible explanations for the existence of residual B cells: either B cells recombine and somehow do not express lethal amounts of toxin, or the cells escape recombination. Southern blot analysis of genomic DNA from MACS-enriched splenic B-cell fractions revealed that the vast majority of surviving B cells did not undergo Cre recombination (unpublished data). As we did not detect any mutations in the *loxP* sites (data not shown), we favor the hypothesis that surviving B cells do not express functional amounts of Cre. Additionally, a significant increase in the number of BrdU-positive B cells in mutant animals (Fig. 3E) is indicative of a higher turnover of the B-cell pool in double-heterozygous animals. Based on these experimental findings, we propose the following scenario. While Cre-recombined B-cells are eliminated, some cells escape recombination, and the B-cell pool is replenished by positive selection. All together, our data show that the depletion system is functional and cell type specific in liver and B cells.

Depletion of cortical neurons with Nex-Cre mice. Next, we were interested in depleting specific cell types in the central nervous system (CNS) and there analyzed depletion and depletion kinetics in great detail. In the Nex-Cre line, the Cre ORF was inserted by a knockin strategy into the *nex* locus, thereby ensuring Nex-specific expression of Cre (S. Goebbels and K. A. Nave, personal communication). Nex is a basic helix-loop-helix transcription factor that is predominantly expressed in pyramidal, postmitotic neurons from E11.5 in the future cortical plate (4, 34, 35). When we crossed mice from our R26:LacZ/DT-A line with the Nex-Cre mice, double-heterozygous, mutant mice were born but died unexpectedly within the first day. Therefore, we focused our analysis on embryonic stages and studied the time course and the degree of depletion. To this end, we performed detailed immunohistochemical and histological analyses of brain sections. At E12.5, 24 h after the onset of Cre expression, no significant differences in the numbers of Cre-positive (Fig. 4A and B) and TUNEL-positive (results not shown) cells were apparent, when mutant (R26:LacZ/DT-A Nex-Cre double-heterozygous) embryos and

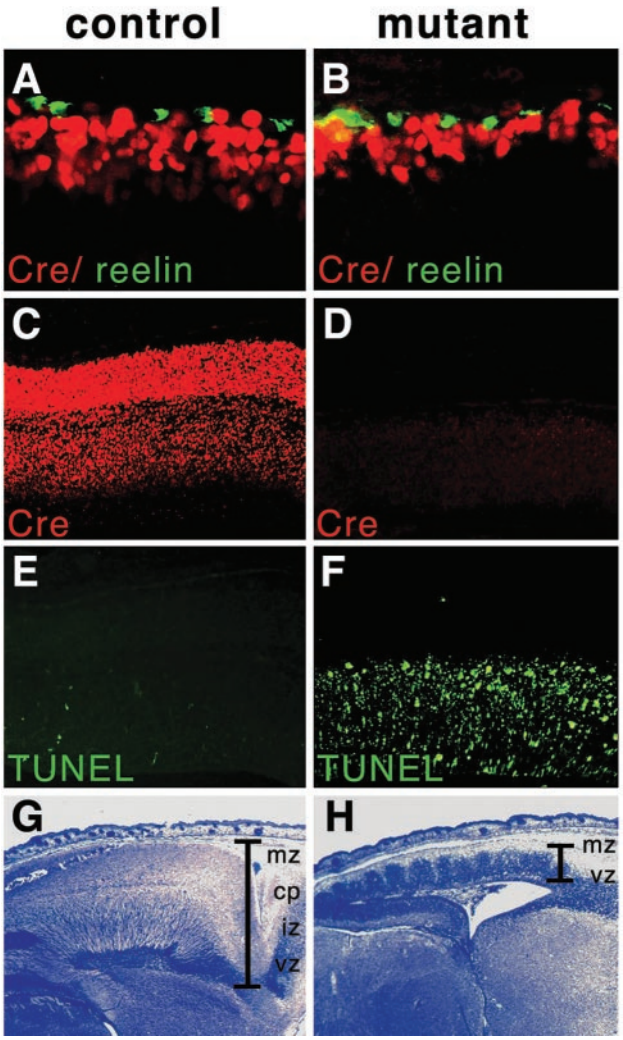

FIG. 4. Depletion of cortical neurons. (A and B) Immunohistochemical analyses of E12.5 embryo cortices with Cre-specific (red) and reelin-specific (green) antibodies. Note the slightly thinner layer of Cre-positive cells in the mutant cells (B) adjacent to the reelin-expressing cells. (C and D) Immunohistochemical analyses of E16.5 embryo cortices with a Cre-specific antibody. Note the almost complete absence of immunoreactivity in the mutant cortex (D) compared to the distinct staining in the different layers from the control cortex (C). (E and F) TUNEL analysis of sections from E16.5 cortices. In the control section, only a few positive cells could be detected in the intermediate zone and cortical plate (E), while the vast majority of cells was labeled in sections from mutants (F). (G and H) Histological analyses of E18.5 embryos. Note the abnormal wavelike structure emerging from the ventricular zone in the extremely thin mutant cortex (H) compared to the normal layering of the control cortex (G). The different layers are indicated. mz, marginal zone; cp, cortical plate; iz, intermediate zone; vz, ventricular. In results not shown here, *lacZ* staining of sagittally sectioned vibratome slices revealed regular migration of unrecombined (*lacZ*-positive) subventricular cells into the intermediate zone, where the absence of *lacZ* staining demonstrates that Cre-mediated recombination had already occured, unlike the regular *lacZ* pattern in the normally layered cortex of the control section.

control (Nex-Cre single-transgene) embryos were compared. Although the Cre-expressing cells in mutants seemed slightly unorganized and slightly decreased in number, they were detected adjacent to the reelin-producing layer of Cajal-Retzius cells, demonstrating a normal layering of the cortex at this developmental stage (Fig. 4B). Two days later, we found a dramatic increase in TUNEL-positive cells in the mutants in sharp contrast to the controls, where no TUNEL-positive cells could be detected and the Cre-expressing neuronal layer was expanding (data not shown). This result is in good agreement with our in vitro findings with Cre-transfected ES cells. So apparently the time required from the onset of Cre expression to recombination of the *loxP*-flanked allele and accumulation of toxic amounts of DT-A is roughly between 36 and 48 h. At E16.5 in control animals, almost no TUNEL-positive cells could be detected within the Cre-expressing neurons of the intermediate zone and cortical plate (Fig. 4C and E). In mutant animals, however, the cortex was then filled with a high number of TUNEL-positive, apoptotic cells and virtually lacked Cre expression (Fig. 4D and F). At E18.5, the cortex showed the typical characteristic layering in the wild type (Fig. 4G), while the toxin-induced dying of cortical neurons resulted in a completely degenerated thin cortex with abnormal layering and a unique wavelike structure in the mutant mouse cortical cells (Fig. 4H). This structure seemed to be caused by the immigration of proliferating Nex-negative, and thus *lacZ*-positive, precursors into the intermediate zone comprised of apoptotic, *lac*Z-negative cells (results not shown). These experiments clearly demonstrate that postmitotic cortical neurons could effectively be killed by Nex-Cre-induced DT-A expression.

Deletion of myelinating glial cells with CNP-Cre mice. To delete myelinating glia cells, the R26:LacZ/DT-A strain was crossed to heterozygous CNP-Cre (knockin) mice, in which Cre is expressed under the control of both existing endogenous 2′3′-cyclo-nucleotide 3′-phosphodiesterase (CNP) promoters (19). CNP is already detectable in oligodendrocyte precursors as early as E11.5 to 12, when these precursors are identifiable by their Olig2, Olig1, or sox10 expression; CNP is maintained in mature oligodendrocytes. To a much lesser extent, Schwann cells also express CNP (5, 37). Myelination of the CNS is a process that predominantly takes place during the first three postnatal weeks and is accompanied by a highly proliferative phase of oligodendrocytes and precursors (11). Double mutant offspring developed normally until postnatal day (P) 8 to 10 but thereafter showed whole-body tremors and a characteristic weakness of the hind legs. In contrast to their littermates, these double mutant offspring began to lose weight and died between P12 and 14. To analyze oligodendrocyte development and maturation in these mice, we performed a detailed immunohistochemical analysis of brain sections by using a variety of oligodendrocyte-, myelin-, and Cre-specific antibodies (MAG, MBP, and Cre) (Fig. 5) and CNP-specific antibodies (results not shown). Strikingly, we were unable to detect any immunoreactivity in brain sections from mutant animals at any time point investigated (P0 to 14) (Fig. 5). This result was also confirmed at the RNA level by in situ hybridization with a digoxigenin-labeled, MBP-specific probe. In contrast, the patterns for GFAP-positive astrocytes (Fig. 5F) and NF160-positive neurites (data not shown) were not affected. The depletion of oligodendrocytes was also confirmed at the histological level (data not shown). Except for some scarce MBP signals in rare sections from spinal cord (data not shown), we therefore conclude that the depletion was complete and consequently was associated with a complete lack of myelination in those animals.

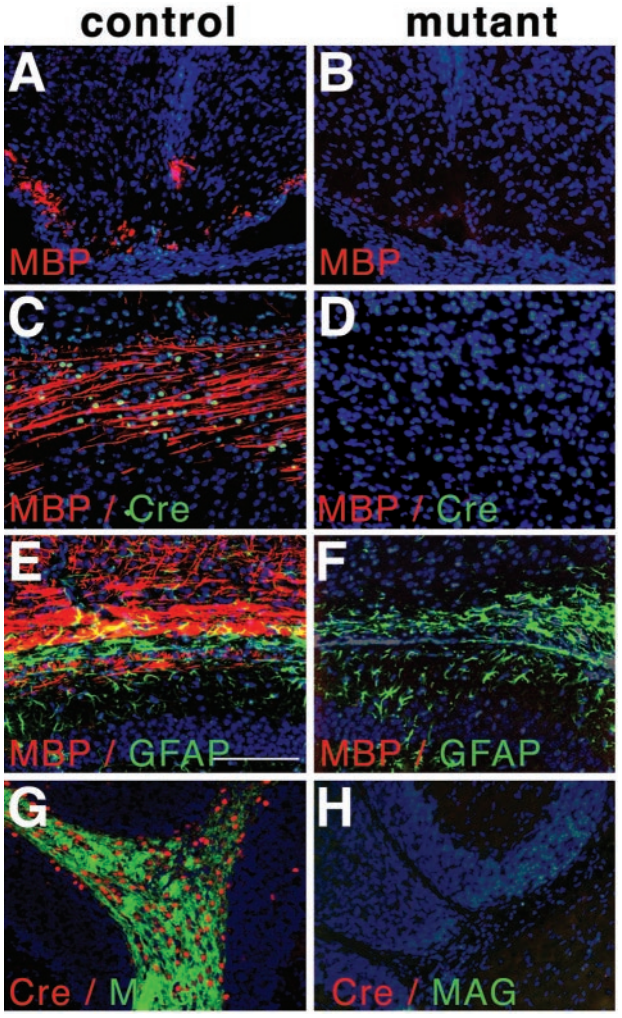

FIG. 5. Depletion of oligodendrocytes. (A and B) Immunofluorescence analysis with MBP-specific antibodies of spinal cord sections from early postnatal animals. Note the presence of staining in the control tissue at ventrolateral positions and absence of staining in the mutant tissue. (C and D) CNS sections from P3 animals analyzed with MBP-specific (red) and Cre-specific (green) antibodies. Note the colocalized expression of Cre and MBP and the absence of staining in the mutant. (E-H) Immunofluorescent analyses of P14 animals, showing parts of the corpus callosum (E and F) and cerebellum (G and H). Analysis with GFAP-specific (green) and MBP-specific (red) antibodies revealed normal staining for GFAP in the mutant but an absence of MPB expression (F). Cre-specific (red) and MAG-specific (green) antibodies revealed the colocalization of both antigens in the cerebellum of the control (G) and complete absence in corresponding sections from the mutant (H).

As CNP is also expressed in Schwann cells, although at lower levels, we analyzed sciatic nerves by light and electron microscopy for morphological changes. In mutant animals, the numbers of myelinated fibers in the nerves were drastically reduced in comparison to nerves of control animals; however, some myelinated axons did occur (Fig. 6A and B). Another charac-

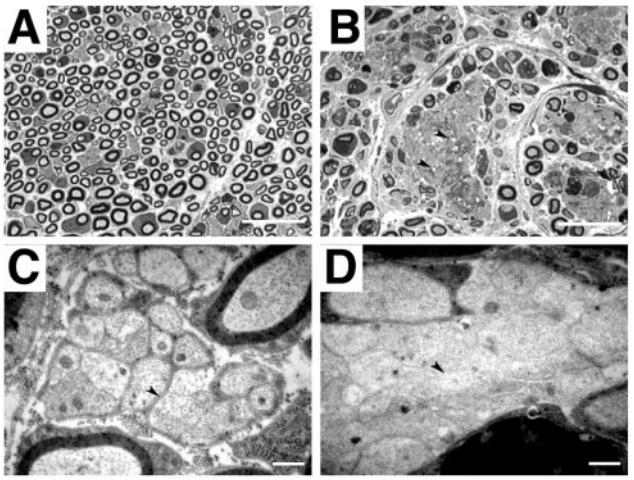

FIG. 6. Schwann cell ablation in the sciatic nerve. (A and B) Histological analyses of semithin sections from control (A) and mutant (B) sciatic nerves, showing large areas of unmyelinated axons next to apparently normally myelinated axons (B). (C and D) Higher magnification revealed that axons were in direct contact with each other (arrowhead, D) and not separated by Schwann cell cytoplasm as in unmyelinated control axons (arrowhead, C). Very often, axons showed clear signs of degeneration, such as vacuoles and electron-dense plaques. Scale bars, 40 μm (A and B) and 2 μm (C and D).

teristic feature of affected nerves was the abnormal occurrence of large clusters of unmyelinated axons (Fig. 6B) that often showed signs of axonal degeneration, which probably occurs secondary to the loss of Schwann cell support (9, 30). Higher magnification revealed that axons, which seemed to be a mixed population of small and large calibers within these large clusters, were not surrounded by Schwann cell cytoplasm (Fig. 6D). In the peripheral nervous system, CNP is expressed in myelinating and nonmyelinating Schwann cells; however, CNP-negative Schwann cells also exist (39). This expression pattern in the peripheral nervous system fits in very well with the phenotypes observed in the Schwann cell population, where apparently normal and aberrant axons reside within the same nerve. Interestingly, similar phenotypes in mice carrying a transgene encoding DT-A under the control of the Schwann cell-specific P_0 promoter have been described, where toxin expression did not comprise the whole Schwann cell population (25).

In summary, we describe here the generation of a universal depletion system based on an inducible DT-A allele. We created a mouse line (R26:LacZ/DT-A) that carries a silenced $lacZ^{flox}$–DT-A cassette incorporated into the ubiquitously expressed ROSA26 locus. This locus is well known for its stable and ubiquitous expression of transgenes as well as for its applicability in Cre-mediated recombination (36). We show here that the R26:LacZ/DT-A mouse line can be used to deplete cells within a wide range of tissues. The degree of depletion was found to be dependent on the regenerative capacity of the depleted tissue and the percentage of Cre-positive cells in a given tissue and can include the entire population (e.g., oligodendrocytes). The major advantages of our system are its broad applicability to a wide spectrum of cell types and developmental stages and the possibility of having founder lines that are themselves phenotypically normal and generate very reproducible phenotypes in the F1 generation. For every Cre line used, the exact expression pattern and expression level have to be determined to ensure that the desired degree of ablation can be achieved. The time required from onset of Cre expression to elimination of the recombined cells is approximately 2 days. When adult phenotypes are analyzed, this time scale is acceptable. However, for depletion experiments during embryogenesis, the time course has to be critically considered, depending on the cell type or tissue to be analyzed. Due to the strong negative effect of DT-A on the translation machinery, a rapidly dividing precursor is significantly slowed down much sooner than apoptosis is detectable. Also, cells that secrete factors will not function properly much earlier. Cells expressing surface molecules implicated in signaling processes might be problematic, as the signal persists until the cell is completely removed. In contrast to depletion due to herpes simplex thymidine kinase, which is restricted to proliferating cells, depletion due to DT-A is not dependent on the cell cycle. No administration of a second component is required, which might be a problem for other previously reported systems, because of dependence on blood circulation or the presence of biological barriers (placenta or blood-brain barrier) (23, 32). To model human diseases and to study regeneration, partial and repeated cell depletions might be desired. For this, an enlarged temporal control over our system could be accomplished by using Cre lines with inducible Cre expression or viruses that confer Cre expression on infected cells (20). As the elimination of endogenous tissues is genetically controlled, exogenous tissues will not be affected by depletion; therefore, our model will offer new opportunities for stem cell research, as the regenerative potential of cells or tissues can be studied by transplantations into cell-depleted animals.

ACKNOWLEDGMENTS

We thank Uta Grieshammer, Gail Martin, and Phil Soriano for the gift of plasmids and probes; Klaus Rajewsky, Günter Schütz, and Christian Trautwein for the provision of mouse lines; and Alex Scheffold and Andreas Radbruch for help with the FACS analysis.

Work in D.R.'s laboratory was supported by the DFG (SFB 444) and the BMBF (01GS0119; NGFN).

REFERENCES

1. **Amiel, J., and S. Lyonnet.** 2001. Hirschsprung disease, associated syndromes, and genetics: a review. J. Med. Genet. **38:**729–739.
2. **Argos, P., A. Landy, K. Abremski, J. B. Egan, E. Haggard-Ljungquist, R. H. Hoess, M. L. Kahn, B. Kalionis, S. V. Narayana, L. S. Pierson III, et al.** 1986. The integrase family of site-specific recombinases: regional similarities and global diversity. EMBO J. **5:**433–440.
3. **Awatramani, R., P. Soriano, J. J. Mai, and S. Dymecki.** 2001. An Flp indicator mouse expressing alkaline phosphatase from the ROSA26 locus. Nat. Genet. **29:**257–259.
4. **Bartholoma, A., and K. A. Nave.** 1994. NEX-1: a novel brain-specific helix-loop-helix protein with autoregulation and sustained expression in mature cortical neurons. Mech. Dev. **48:**217–228.
5. **Chandross, K. J., R. I. Cohen, P. Paras, Jr., M. Gravel, P. E. Braun, and L. D. Hudson.** 1999. Identification and characterization of early glial progenitors using a transgenic selection strategy. J. Neurosci. **19:**759–774.
6. **Collier, R. J.** 1975. Diphtheria toxin: mode of action and structure. Bacteriol. Rev. **39:**54–85.
7. **Collier, R. J.** 2001. Understanding the mode of action of diphtheria toxin: a perspective on progress during the 20th century. Toxicon **39:**1793–1803.
8. **Davis, B. R., and G. Zauli.** 1995. Effect of human immunodeficiency virus infection on haematopoiesis. Bailliere's Clin. Haematol. **8:**113–130.
9. **de Waegh, S. M., V. M. Lee, and S. T. Brady.** 1992. Local modulation of neurofilament phosphorylation, axonal caliber, and slow axonal transport by myelinating Schwann cells. Cell **68:**451–463.
10. **Farley, F. W., P. Soriano, L. S. Steffen, and S. M. Dymecki.** 2000. Widespread recombinase expression using FLPeR (flipper) mice. Genesis **28:**106–110.

11. **Foran, D. R., and A. C. Peterson.** 1992. Myelin acquisition in the central nervous system of the mouse revealed by an MBP-LacZ transgene. J. Neurosci. **12:**4890–4897.
12. **Friedrich, G., and P. Soriano.** 1991. Promoter traps in embryonic stem cells: a genetic screen to identify and mutate developmental genes in mice. Genes Dev. **5:**1513–1523.
13. **Grieshammer, U., M. Lewandoski, D. Prevette, R. W. Oppenheim, and G. R. Martin.** 1998. Muscle-specific cell ablation conditional upon Cre-mediated DNA recombination in transgenic mice leads to massive spinal and cranial motoneuron loss. Dev. Biol. **197:**234–247.
14. **Hoess, R. H., M. Ziese, and N. Sternberg.** 1982. P1 site-specific recombination: nucleotide sequence of the recombining sites. Proc. Natl. Acad. Sci. USA **79:**3398–3402.
15. **Horcher, M., A. Souabni, and M. Busslinger.** 2001. Pax5/BSAP maintains the identity of B cells in late B lymphopoiesis. Immunity **14:**779–790.
16. **Kellendonk, C., C. Opherk, K. Anlag, G. Schutz, and F. Tronche.** 2000. Hepatocyte-specific expression of Cre recombinase. Genesis **26:**151–153.
17. **Klinge, O.** 1973. Cytologic and histologic aspects of toxically induced liver reactions. Curr. Top. Pathol. **58:**91–116.
18. **Lakso, M., B. Sauer, B. Mosinger, Jr., E. J. Lee, R. W. Manning, S. H. Yu, K. L. Mulder, and H. Westphal.** 1992. Targeted oncogene activation by site-specific recombination in transgenic mice. Proc. Natl. Acad. Sci. USA **89:**6232–6236.
19. **Lappe-Siefke, C., S. Goebbels, M. Gravel, E. Nicksch, J. Lee, P. E. Braun, I. R. Griffiths, and K. A. Nave.** 2003. Disruption of Cnp1 uncouples oligodendroglial functions in axonal support and myelination. Nat. Genet. **33:**366–374.
20. **Lewandoski, M.** 2001. Conditional control of gene expression in the mouse. Nat. Rev. Genet. **2:**743–755.
21. **Lobe, C. G., K. E. Koop, W. Kreppner, H. Lomeli, M. Gertsenstein, and A. Nagy.** 1999. Z/AP, a double reporter for cre-mediated recombination. Dev. Biol. **208:**281–292.
22. **Lozano, A. M., A. E. Lang, W. D. Hutchison, and J. O. Dostrovsky.** 1998. New developments in understanding the etiology of Parkinson's disease and in its treatment. Curr. Opin. Neurobiol. **8:**783–790.
23. **Mallet, V. O., C. Mitchell, J. E. Guidotti, P. Jaffray, M. Fabre, D. Spencer, D. Arnoult, A. Kahn, and H. Gilgenkrantz.** 2002. Conditional cell ablation by tight control of caspase-3 dimerization in transgenic mice. Nat. Biotechnol. **20:**1234–1239.
24. **Mao, X., Y. Fujiwara, and S. H. Orkin.** 1999. Improved reporter strain for monitoring Cre recombinase-mediated DNA excisions in mice. Proc. Natl. Acad. Sci. USA **96:**5037–5042.
25. **Messing, A., R. R. Behringer, J. P. Hammang, R. D. Palmiter, R. L. Brinster, and G. Lemke.** 1992. P0 promoter directs expression of reporter and toxin genes to Schwann cells of transgenic mice. Neuron **8:**507–520.
26. **Nagy, A.** 2000. Cre recombinase: the universal reagent for genome tailoring. Genesis **26:**99–109.
27. **Palmiter, R. D., R. R. Behringer, C. J. Quaife, F. Maxwell, I. H. Maxwell, and R. L. Brinster.** 1987. Cell lineage ablation in transgenic mice by cell-specific expression of a toxin gene. Cell **50:**435–443.
28. **Pasparakis, M., M. Schmidt-Supprian, and K. Rajewsky.** 2002. IκB kinase signaling is essential for maintenance of mature B cells. J. Exp. Med. **196:**743–752.
29. **Rickert, R. C., J. Roes, and K. Rajewsky.** 1997. B lymphocyte-specific, Cre-mediated mutagenesis in mice. Nucleic Acids Res. **25:**1317–1318.
30. **Riethmacher, D., E. Sonnenberg-Riethmacher, V. Brinkmann, T. Yamaai, G. R. Lewin, and C. Birchmeier.** 1997. Severe neuropathies in mice with targeted mutations in the ErbB3 receptor. Nature **389:**725–730.
31. **Rinkenberger, J. L., and S. J. Korsmeyer.** 1997. Errors of homeostasis and deregulated apoptosis. Curr. Opin. Genet. Dev. **7:**589–596.
32. **Saito, M., T. Iwawaki, C. Taya, H. Yonekawa, M. Noda, Y. Inui, E. Mekada, Y. Kimata, A. Tsuru, and K. Kohno.** 2001. Diphtheria toxin receptor-mediated conditional and targeted cell ablation in transgenic mice. Nat. Biotechnol. **19:**746–750.
33. **Schwab, M. H., A. Bartholomae, B. Heimrich, D. Feldmeyer, S. Druffel-Augustin, S. Goebbels, F. J. Naya, S. Zhao, M. Frotscher, M. J. Tsai, and K. A. Nave.** 2000. Neuronal basic helix-loop-helix proteins (NEX and BETA2/Neuro D) regulate terminal granule cell differentiation in the hippocampus. J. Neurosci. **20:**3714–3724.
34. **Schwab, M. H., S. Druffel-Augustin, P. Gass, M. Jung, M. Klugmann, A. Bartholomae, M. J. Rossner, and K. A. Nave.** 1998. Neuronal basic helix-loop-helix proteins (NEX, neuroD, NDRF): spatiotemporal expression and targeted disruption of the NEX gene in transgenic mice. J. Neurosci. **18:**1408–1418.
35. **Shimizu, C., C. Akazawa, S. Nakanishi, and R. Kageyama.** 1995. MATH-2, a mammalian helix-loop-helix factor structurally related to the product of Drosophila proneural gene atonal, is specifically expressed in the nervous system. Eur. J. Biochem. **229:**239–248.
36. **Soriano, P.** 1999. Generalized lacZ expression with the ROSA26 Cre reporter strain. Nat. Genet. **21:**70–71.
37. **Sprinkle, T. J.** 1989. 2′,3′-cyclic nucleotide 3′-phosphodiesterase, an oligodendrocyte-Schwann cell and myelin-associated enzyme of the nervous system. Crit. Rev. Neurobiol. **4:**235–301.
38. **Stobrawa, S. M., T. Breiderhoff, S. Takamori, D. Engel, M. Schweizer, A. A. Zdebik, M. R. Bosl, K. Ruether, H. Jahn, A. Draguhn, R. Jahn, and T. J. Jentsch.** 2001. Disruption of ClC-3, a chloride channel expressed on synaptic vesicles, leads to a loss of the hippocampus. Neuron **29:**185–196.
39. **Yuan, X., R. Chittajallu, S. Belachew, S. Anderson, C. J. McBain, and V. Gallo.** 2002. Expression of the green fluorescent protein in the oligodendrocyte lineage: a transgenic mouse for developmental and physiological studies. J. Neurosci. Res. **70:**529–545.
40. **Zambrowicz, B. P., A. Imamoto, S. Fiering, L. A. Herzenberg, W. G. Kerr, and P. Soriano.** 1997. Disruption of overlapping transcripts in the ROSA beta geo 26 gene trap strain leads to widespread expression of beta-galactosidase in mouse embryos and hematopoietic cells. Proc. Natl. Acad. Sci. USA **94:**3789–3794.